JMEPEG (2012) 21:2303–2315
DOI: 10.1007/s11665-012-0190-7

1059-9495/$19.00

Optimizing Diffusion Bonding Parameters in AA6061-T6 Aluminum and AZ80 Magnesium Alloy Dissimilar Joints

M. Joseph Fernandus, T. Senthilkumar, V. Balasubramanian, and S. Rajakumar

(Submitted June 14, 2011; in revised form January 9, 2012)

The main difficulty when joining magnesium (Mg) and aluminum (Al) alloys by fusion welding lies in the formation of oxide films and brittle intermetallic in the bond region which affects the integrity of the joints. However, diffusion bonding is a suitable process to join these two materials as no such characteristic defects are produced at the joints. The diffusion bonding process parameters such as bonding temperature, bonding pressure, holding time, and surface roughness of the specimen play a major role in determining the joint strength. In this investigation, an attempt was made to develop empirical relationships to predict the strengths of diffusion bonded AZ80 magnesium and AA6061 aluminum alloys dissimilar joints from the process parameters based on central composite factorial design. Response surface methodology was applied to optimize the process parameters to attain the maximum shear strength and bonding strength of the joint. From this investigation, it was found that the bonds produced with the temperature of 405.87 °C, pressure of 7.87 MPa, holding time of 29.02 min and surface roughness of 0.10 μm exhibited maximum shear strength and bonding strength of 57.70 and 76.90 MPa, respectively. The intermetallic formation at the interface was identified.

Keywords aluminum alloy, diffusion bonding, magnesium alloy, response surface methodology, strength

1. Introduction

The magnesium (Mg) and aluminum (Al) alloys are used in wide variety of aerospace structural applications due to some unique performance such as low density, high specific strength, and good ductility (Ref 1). The application of magnesium and its alloys is extended from navigation and military affairs fields to civil products of high additional value such as automobile, computer, and communication equipment. Dissimilar welding of magnesium and aluminum alloys would achieve weight reduction and high efficiency of production by a substitution of Mg alloy for Al alloy (Ref 2).

However, the refractory oxide film of Mg and Al results in inclusions at the weld metal. Moreover, the conventional fusion welding technique causes severe thermal cracking and easy formation of brittle intermetallic in the joints produced. Therefore, the welding of Mg and Al dissimilar materials by the fusion welding method is very difficult (Ref 3). Hence, the diffusion bonding technique is used to join these materials (Ref 4).

The predominant process parameters in diffusion bonding process are: (bonding) temperature, (bonding) pressure, and (holding) time (Ref 5). Other important parameter is surface roughness of the materials to be joined (Ref 6). From the literature review (Ref 1, 2, 7-9) it is understood that the most of the published information on diffusion bonding of magnesium and aluminum dissimilar materials focused on microstructure analysis, phase formation studies, hardness survey at the interface to evaluate the subsequent influence on strength and the processing map to find out the good quality bond. All the above-mentioned investigation was carried out on trial basis to attain optimum bonding conditions. Only few research works have been reported (Ref 10, 11) to optimize the diffusion bonding parameters to attain maximum shear strength and bonding strength of dissimilar joints. To obtain the maximum strength, it is essential to have complete control over the relevant process parameters.

Various prediction methods can be applied to define the desired output variables through developing mathematical models to specify the relationship between the input parameters and the output variables. The response surface methodology (RSM) is helpful in developing a suitable approximation for the true functional relationship between independent variables and the response variable that may characterize the nature of the joints (Ref 12). It has been proved by several researchers that efficient use of statistical design of experimental techniques allows development of an empirical methodology, to incorporate a scientific approach in solid-state procedures such as diffusion bonding (Ref 10, 11, 13) and friction stir welding (Ref 14, 15), and fusion welding procedure (Ref 16-18). Hence, in this investigation an attempt was made to optimize diffusion bonding process parameters to attain maximum shear strength and bonding strength in AZ80 magnesium alloy and AA6061 aluminum alloy dissimilar joints using RSM.

M. Joseph Fernandus, Department of Mechanical Engineering, Srinivasan Engineering College, Perambalur 621 212, Tamil Nadu, India; **T. Senthilkumar**, Department of Mechanical Engineering, Anna University of Technology Tiruchirappalli, Tiruchirappalli 620 024, Tamil Nadu, India; and **V. Balasubramanian** and **S. Rajakumar**, Department of Manufacturing Engineering, Center for Materials Joining and Research (CEMAJOR), Annamalai University, Annamalainagar 608 002, Tamil Nadu, India. Contact e-mails: mjf_me@yahoo.co.in, senthil@tau.edu.in, balasubramanian.v.2784@annamalaiuniversity.ac.in, and srkcemajor@yahoo.com.

2. Experimental Work

Square-shaped specimens (50 × 50 mm) were machined from rolled plates of 10 mm thick magnesium (AZ80) and 6 mm thick aluminum (AA6061) alloys. The chemical composition of the base metals used in this investigation is shown in Table 1. From the literature, the predominant factors which are having greater influence on lap shear strength and bonding strength of diffusion bonded joints were identified. They are: (i) bonding temperature, (ii) bonding pressure, (iii) holding time, and (iv) surface roughness. The bonding surfaces of samples were ground flat by 200#, 400#, and 600# grit SiC papers and cleaned in acetone prior to diffusion bonding (Ref 19). Then the polished and chemically treated specimens were stacked in a die made up of 316L stainless steel and experimental set-up for diffusion bonding, shown in Fig. 1, was inserted into a vacuum chamber (vacuum pressure of −29 mm Hg was maintained). The specimens were heated up to the bonding temperature using induction furnace with a heating rate of 25 °C/min, simultaneously the required pressure was applied. After the completion of bonding, the samples were cooled to room temperature before removal from the chamber.

The experiments were conducted to determine the working range of the above factors. Feasible limits of the parameters were chosen in such a way that the diffusion bonds should be free from any visual defects. The important factors that are influencing the lap shear strength and bonding strength of diffusion bonding and their working range for AZ80 magnesium alloy and AA6061 aluminum alloy are presented in Table 2.

As the range of individual factor was wide, a central composite rotatable four-factor, five-level factorial design matrix was selected. The experimental design matrix (Table 3) consisting 30 sets of coded condition and comprising a full replication four-factor factorial design of 16 points, 8 star points, and 6 center points was used. The upper and lower limits of the parameters were coded as +2 and −2, respectively. The coded values for intermediate levels can be calculated from the relationship.

$$X_i = 2[2X - (X_{\max} + X_{\min})]/(X_{\max} - X_{\min}) \quad \text{(Eq 1)}$$

where X_i is the required coded value of a variable X and X is any value of the variable from $X_{\min}$ to $X_{\max}$. The bonds were made as per the conditions dictated by the design matrix at random order so as to avoid the noise creeping output response.

As the joints were not large enough for normal lap shear strength and bond strength testing, a non-standard test was devised to measure the shear strength of the bonds. The dimensions of lap shear tensile specimen and ram tensile specimen are shown in Fig. 2(a) and (b), respectively. The ram tensile test set-up is shown in Fig. 2(c). The bonded specimens were prepared from the Mg/Al diffusion bonded joints by a wire-cut electric discharge machine (WEDM). The lap shear tensile test and bond strength test were carried out in 100 kN capacity servo controlled Universal Testing Machine. The photograph of ram tensile test specimen is shown in Fig. 2(d). Microstructure analysis was carried out using a light optical microscope. The magnesium side was etched with a solution containing ethanol, picric acid, acetic acid, and water whereas the aluminum side was etched with Keller's solution. The optical micrographs of interface region of Mg-Al for different joints are shown in Fig. 3. The micrograph contains base metals of aluminum and magnesium, transition region of aluminum and magnesium regions and mid-diffusion. Energy dispersive spectrum (EDS) analysis was taken at the interface of a joint no. 23 and the results are presented in Fig. 4(a) and (b). Interface contains 37.97% of magnesium, 60.80% of aluminum, and

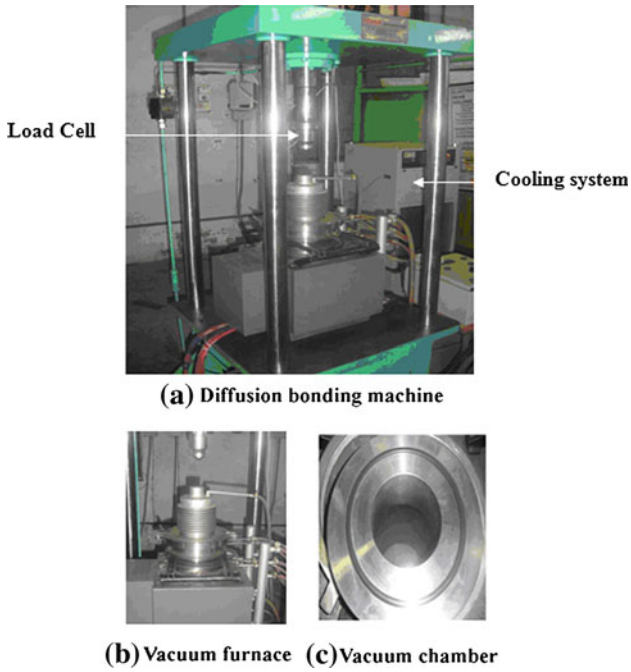

Fig. 1 Experimental set-up for diffusion bonding. (a) Diffusion bonding machine, (b) vacuum furnace, and (c) vacuum chamber

Table 2 Feasible working limits of diffusion bonding parameters

S. no.	Parameters	Notation	Unit	Levels				
				−2	−1	0	1	2
1.	Bonding temperature	T	°C	375	390	405	420	435
2.	Bonding pressure	P	MPa	5	7.5	10	12.5	15
3.	Holding time	H	min	5	15	25	35	45
4.	Surface roughness	S	μm	0.1	0.2	0.3	0.4	0.5

Table 1 Chemical composition (wt.%) of base metals

	Mg	Si	Ti	Cr	Mn	Fe	Cu	Zn	Pb	Sn	Zr	Al
AA6061-T6	1.0	0.5	0.15	0.1	0.15	0.7	0.2	0.25	…	…	…	96.95
AZ80	91.36	…	…	…	0.101	…	…	0.398	0.005	0.001	Traces	8.140

Table 3 Design matrix and experimental results

Joint numbers	Factors				Shear strength, MPa	Bonding strength, MPa
	T	P	H	S		
1	−1	−1	−1	−1	50	67
2	+1	−1	−1	−1	47	64
3	−1	+1	−1	−1	49	66
4	+1	+1	−1	−1	47	64
5	−1	−1	+1	−1	50	67
6	+1	−1	+1	−1	56	73
7	−1	+1	+1	−1	48	65
8	+1	+1	+1	−1	53	70
9	−1	−1	−1	+1	34	51
10	+1	−1	−1	+1	37	54
11	−1	+1	−1	+1	43	60
12	+1	+1	−1	+1	46	63
13	−1	−1	+1	+1	37	54
14	+1	−1	+1	+1	48	65
15	−1	+1	+1	+1	44	61
16	+1	+1	+1	+1	55	72
17	−2	0	0	0	42	59
18	+2	0	0	0	51	68
19	0	−2	0	0	43	60
20	0	+2	0	0	50	67
21	0	0	−2	0	39	56
22	0	0	+2	0	51	68
23	0	0	0	−2	56	77
24	0	0	0	+2	43	60
25	0	0	0	0	57	74
26	0	0	0	0	55	72
27	0	0	0	0	55	72
28	0	0	0	0	55	72
29	0	0	0	0	48	66
30	0	0	0	0	51	68

1.23% of silicon. X-ray diffraction (XRD) analysis was performed on both sides of the bonds and the results are presented in Fig. 4(c) and (d). The presence of intermetallic phases such as Mg_2Al_3, Mg_3Al_2, MgAl, $Mg_{17}Al_{12}$, $MgAl_2O_4$, and SiO_2 are confirmed from the XRD and EDS analyses.

3. Developing Empirical Relationships

Shear strength and bonding strength of the diffusion bonded joints are represented by SS and BS, respectively. These responses are function of bonding temperature (T), bonding pressure (P), holding time (H), and surface roughness (S) and they can be expressed as

$$SS = f(T, P, H, S) \quad \text{(Eq 2)}$$

$$BS = f(T, P, H, S) \quad \text{(Eq 3)}$$

The second-order polynomial (regression) equation used to represent the response surface Y is given by (Ref 20)

$$Y = b_0 + \Sigma b_i x_i + \Sigma b_{ii} x_i^2 + \Sigma b_{ij} x_i x_j + e_r \quad \text{(Eq 4)}$$

The selected polynomial for shear strength of diffusion bonded AZ80 magnesium and AA6061 aluminum alloy joints could be expressed as

$$\begin{aligned} SS = {} & b_0 + b_1(T) + b_2(P) + b_3(H) + b_4(S) + b_{11}(T^2) \\ & + b_{22}(P^2) + b_{33}(H^2) + b_{44}(S^2) + b_{12}(TP) + b_{13}(TH) \\ & + b_{14}(TS) + b_{23}(PH) + b_{24}(PS) + b_{34}(HS) \end{aligned} \quad \text{(Eq5)}$$

Similarly, the selected polynomial for the bonding strength of diffusion bonded joint is given below

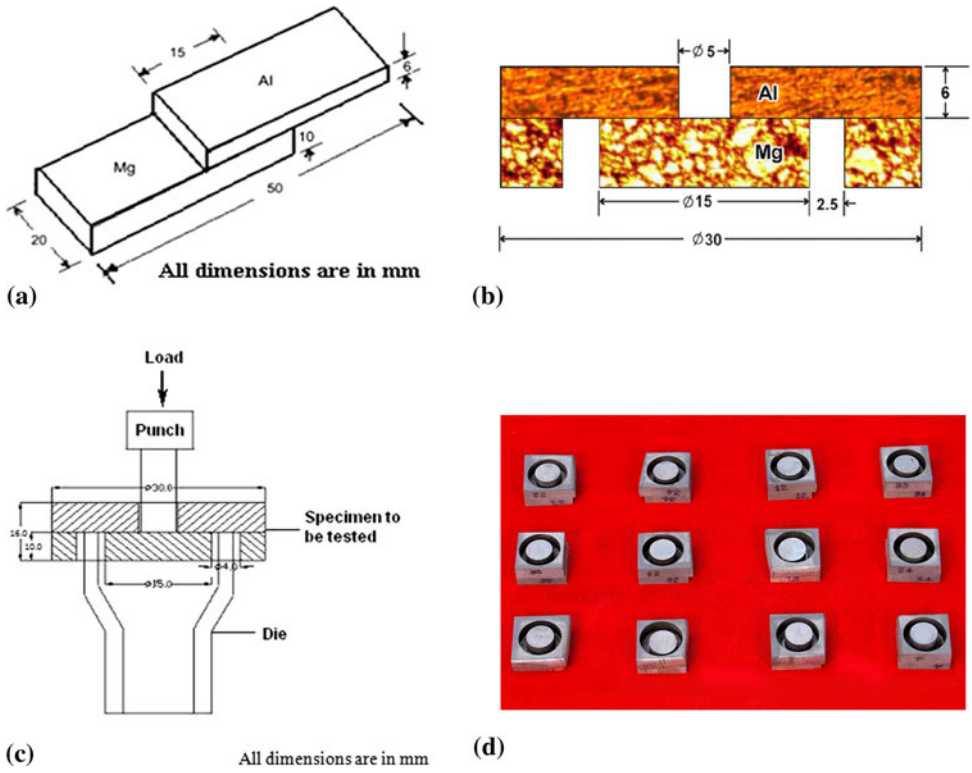

Fig. 2 Experimental details. (a) Dimensions of lap shear tensile specimen, (b) dimensions of ram tensile specimen, (c) Ram tensile test set-up, and (d) Ram tensile specimen photo

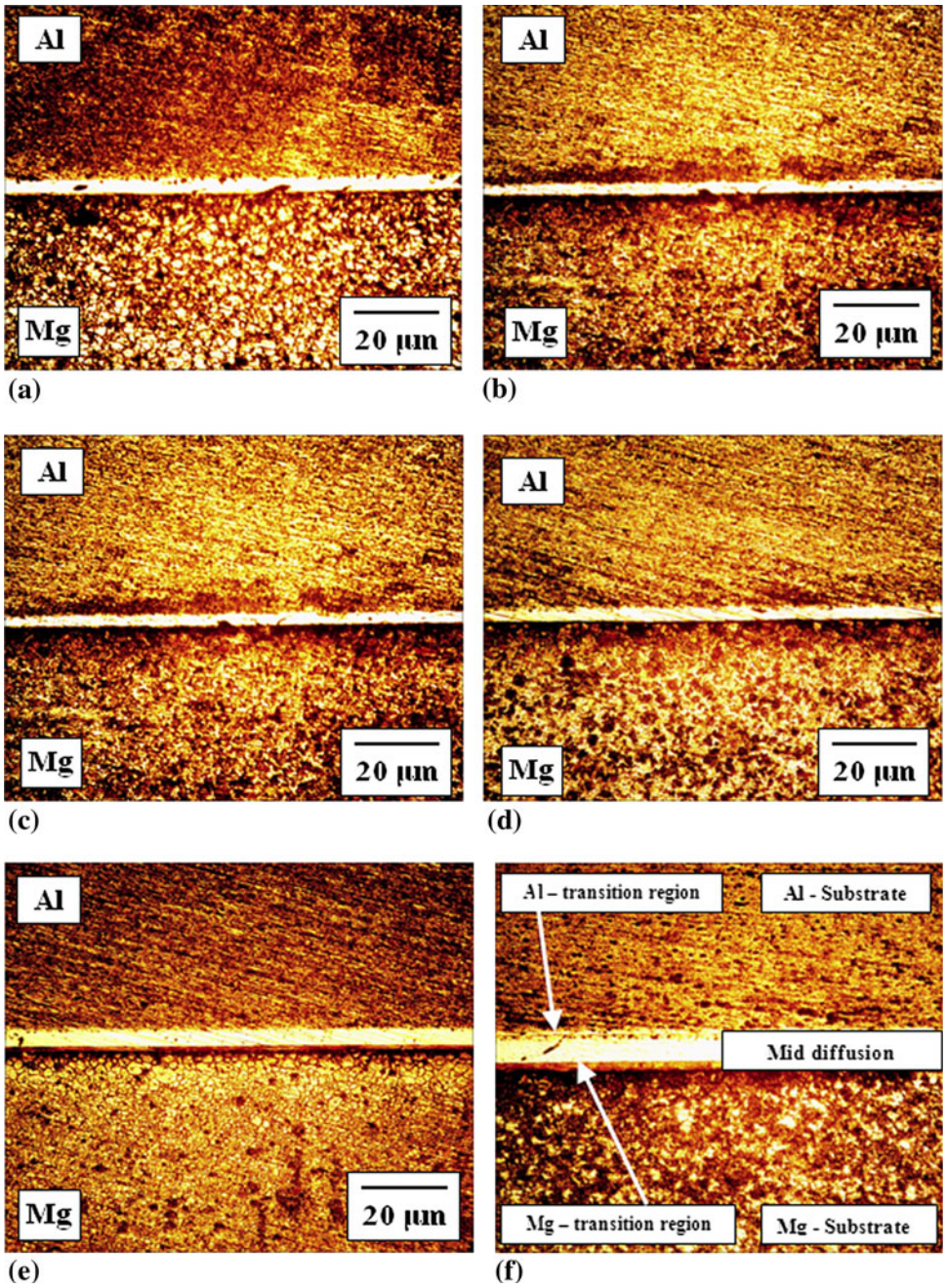

Fig. 3 Optical micrographs at different combinations of process parameters. Joint Nos. (a) 3, (b) 9, (c) 13, (d) 18, (e) 23, and (f) 29

$$\begin{aligned}\mathrm{BS} = {} & b_0 + b_1(T) + b_2(P) + b_3(H) + b_4(S) + b_{11}\left(T^2\right) \\ & + b_{22}\left(P^2\right) + b_{33}\left(H^2\right) + b_{44}\left(S^2\right) + b_{12}(TP) + b_{13}(TH) \\ & + b_{14}(TS) + b_{23}(PH) + b_{24}(PS) + b_{34}(HS)\end{aligned} \quad \text{(Eq 6)}$$

where b_0 is the average of the responses and b_1, b_2, b_3,…, b_{44} are regression coefficients that depend on respective linear, interaction, and squared terms of factors. The value of the coefficient was calculated using Design Expert Software. After determining the significant coefficients at the (95% confidence level), the final models were developed using only these coefficients and the final empirical relationship to estimate shear strength and bonding strength are given below:

$$\begin{aligned}\mathrm{SS} = {} & \{53.50 + 2.17(T) + 1.67(P) + 2.58(H) - 3.42(S) \\ & -1.81\left(T^2\right) - 1.81\left(P^2\right) - 2.19\left(H^2\right) - 1.06\left(S^2\right) \\ & +2.00(TH) + 1.38(TS) - 0.50(PH) + 2.38(PS) \\ & +0.63(HS)\}\ \mathrm{MPa}\end{aligned} \quad \text{(Eq 7)}$$

$$\begin{aligned}\mathrm{BS} = {} & \{70.67 + 2.17(T) + 1.67(P) + 2.58(H) - 3.75(S) \\ & -1.94\left(T^2\right) - 1.94\left(P^2\right) - 2.31\left(H^2\right) - 0.69\left(S^2\right) \\ & +2.00(TH) + 1.38(TS) - 0.50(PH) + 2.38(PS) \\ & +0.63(HS)\}\ \mathrm{MPa}\end{aligned} \quad \text{(Eq 8)}$$

The adequacy of the developed model was tested using the analysis of variance (ANOVA) technique and the results of

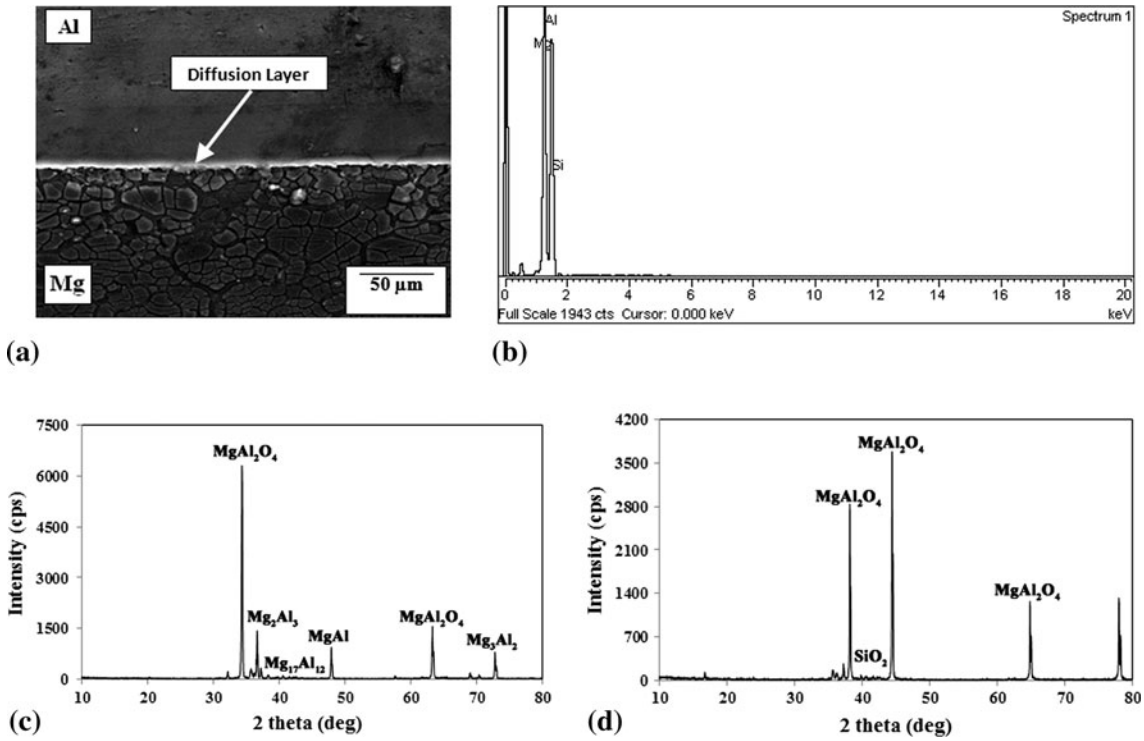

Fig. 4 Microstructural characteristics of AA6061 Al/AZ80 Mg alloy joints. (a) SEM micrograph, (b) EDS results, (c) XRD magnesium side, and (d) XRD aluminium side

Table 4 ANOVA test result for shear strength

Source	Sum of squares	df	Mean square	*F* value	*P* value (prob. > *F*)	
Model	1062.667	14	75.90476	19.18941	<0.0001	Significant
T	112.6667	1	112.6667	28.48315	<0.0001	
P	66.66667	1	66.66667	16.85393	0.0009	
H	160.1667	1	160.1667	40.49157	<0.0001	
S	280.1667	1	280.1667	70.82865	<0.0001	
TP	0	1	0	0	1.0000	
TH	64	1	64	16.17978	0.0011	
TS	30.25	1	30.25	7.647472	0.0144	
PH	4	1	4	1.011236	0.3306	
PS	90.25	1	90.25	22.81601	0.0002	
HS	6.25	1	6.25	1.580056	0.2280	
T^2	90.10714	1	90.10714	22.7799	0.0002	
P^2	90.10714	1	90.10714	22.7799	0.0002	
H^2	131.25	1	131.25	33.18118	<0.0001	
S^2	30.96429	1	30.96429	7.82805	0.0135	
Residual	59.33333	15	3.955556			
Lack of fit	3.833333	10	0.383333	34.256	1.0000	Not significant
Pure error	55.5	5	11.1			
Cor. total	1122	29				

df, degrees of freedom; F, Fisher's ratio; P, probability
SD = 1.98886, mean = 48.00, CV% = 4.143, PRESS = 102, R^2 = 0.947118, adj. R^2 = 0.897762, pred. R^2 = 0.909091, adeq. precision = 15.76201

second-order response surface model fitting in the form of ANOVA are given in Table 4. The determination coefficient (R^2) indicates the goodness of fit for the model. In this case, the value of the determination coefficient (R^2 = 0.9471) indicates that 94.71% of the total variability is explained by the model after considering the significant factors. The models are not over fitted as indicated by the comparison of R^2 and R^2-adjusted values. Only <6% of the total variations are not explained by the model. The value of adjusted determination coefficient (adjusted R^2 = 0.8977) is also high, which indicates a high

Table 5 ANOVA test result for bonding strength

Source	Sum of squares	df	Mean square	*F* value	*P* value (prob. > *F*)	
Model	1147	14	81.92857	22.27665	<0.0001	Significant
T	112.6667	1	112.6667	30.63444	<0.0001	
P	66.66667	1	66.66667	18.12689	0.0007	
H	160.1667	1	160.1667	43.54985	<0.0001	
S	337.5	1	337.5	91.76737	<0.0001	
TP	0	1	0	0	1.0000	
TH	64	1	64	17.40181	0.0008	
TS	30.25	1	30.25	8.225076	0.0117	
PH	4	1	4	1.087613	0.3135	
PS	90.25	1	90.25	24.53927	0.0002	
HS	6.25	1	6.25	1.699396	0.2120	
T^2	102.9643	1	102.9643	27.99633	<0.0001	
P^2	102.9643	1	102.9643	27.99633	<0.0001	
H^2	146.6786	1	146.6786	39.88239	<0.0001	
S^2	12.96429	1	12.96429	3.525032	0.0800	
Residual	55.16667	15	3.677778			
Lack of fit	9.833333	10	0.983333	0.108456	0.9983	Not significant
Pure error	45.33333	5	9.066667			
Cor. total	1202.167	29				

df, degrees of freedom; F, Fisher's ratio; P, probability
SD = 1.917753, mean = 65.17, CV% = 2.942844, PRESS = 121.92, R^2 = 0.954111, adj. R^2 = 0.911281, pred. R^2 = 0.898583, adeq. precision = 18.19

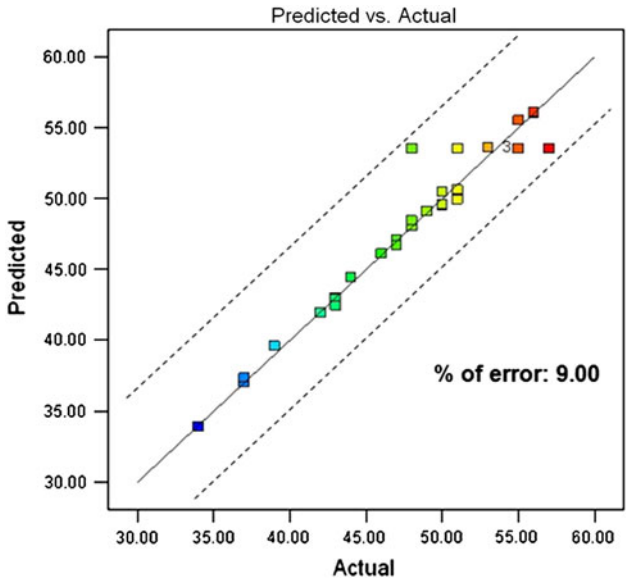

Fig. 5 Normal probability plot of experimental versus predicted shear strength

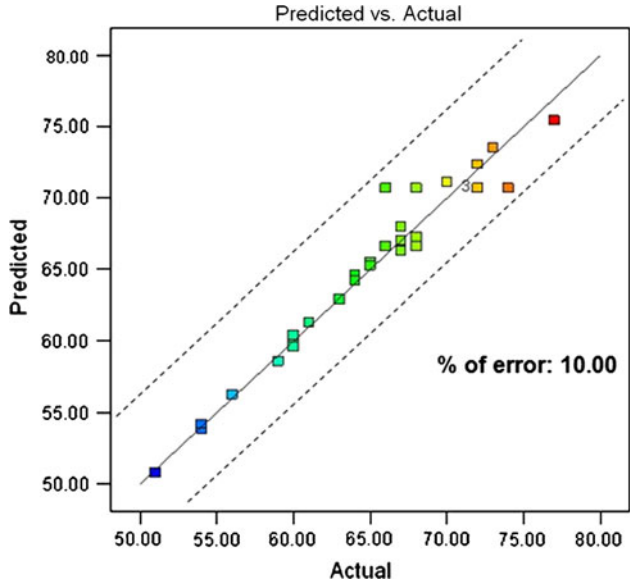

Fig. 6 Normal probability plot of experimental versus predicted bonding strength

significant of the model. Predicted R^2 = 0.9091 is in good agreement with the adjusted R^2 and shows that the model would be expected to explain 90.91% of the variability in new data. A *P* value <0.05 indicated the significant model terms. Value of probability greater than *F* in Table 4 and 5 for the model is <0.05, which indicates that the model is significant. Lack of fit is insignificant and therefore indicates that the model fits well with the experimental data. The high *P* value for the lack of fit test also indicates that the model does adequately fit with the response surface for shear strength. All the above considerations indicate on excellent adequacy of the regression model. Each observed value is compared with the predicted value calculated from the model in Fig. 5 and 6.

4. Optimizing the Diffusion Bonding Parameters

In this investigation, the RSM was used to optimize the diffusion bonding parameters. RSM is a collection of

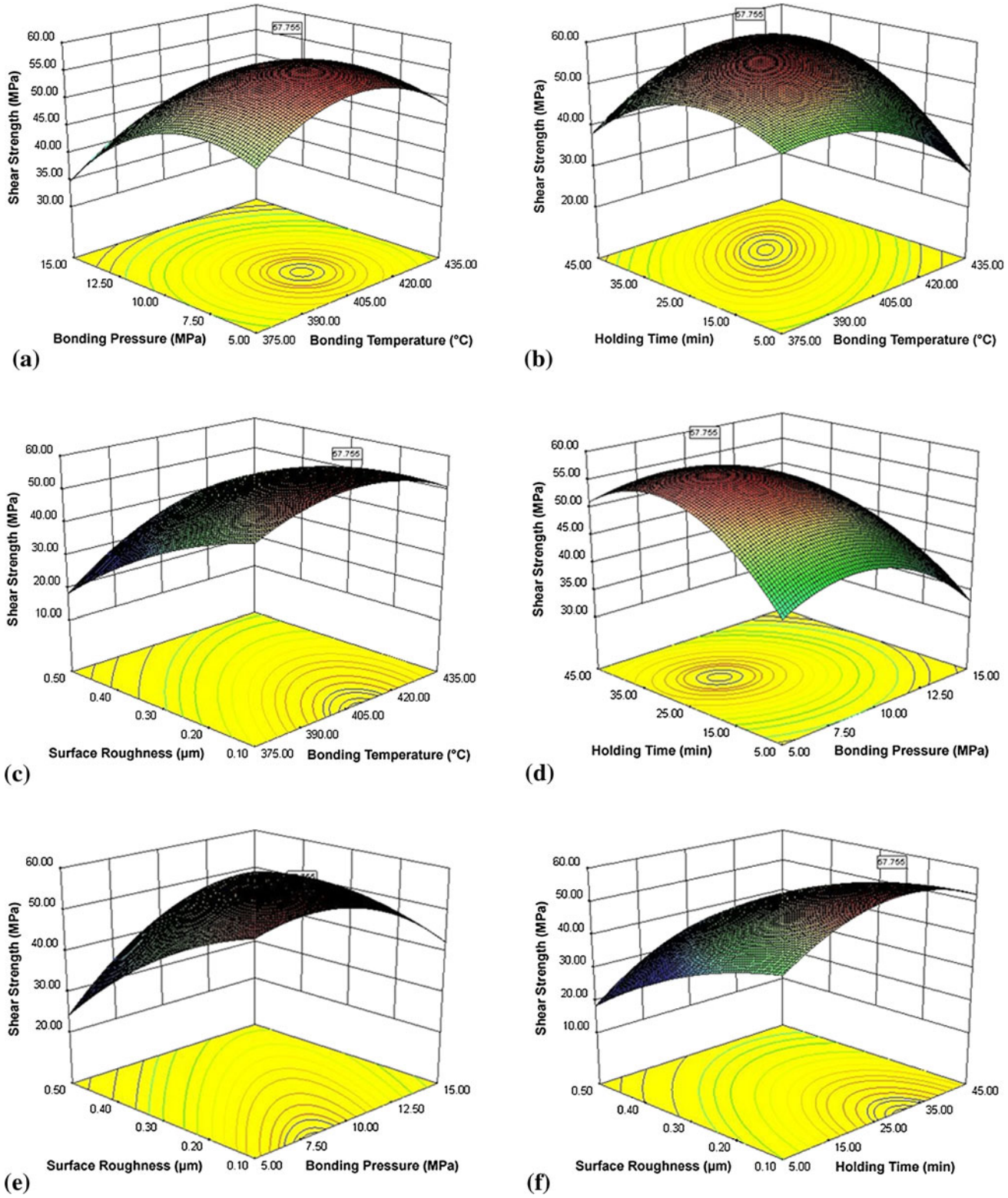

Fig. 7 Response graphs for shear strength

mathematical and statistical techniques that are useful for designing a set of experiments, developing a mathematical model, analyzing for the optimum combination of input parameters, and expressing the values graphically (Ref 16). To obtain the influencing nature and optimized condition of the process on shear strength and bonding strength, the surface plots and contour plots which are the indications of possible independence of factors have been developed for the proposed empirical relation by considering two parameters in the middle level and two parameters in the *X*- and *Y*-axes as shown in

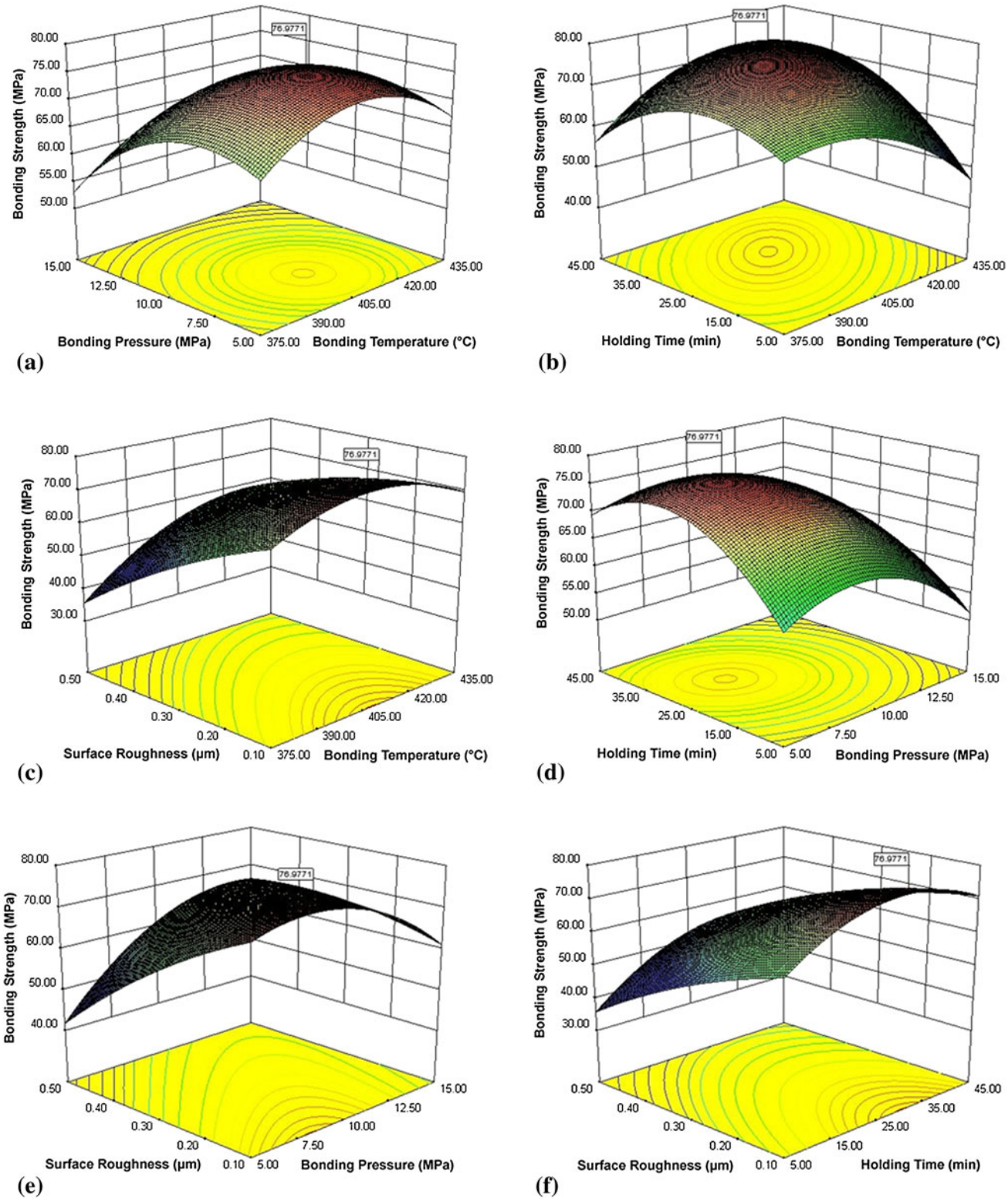

Fig. 8 Response graphs for bonding strength

Fig. 7 and 8 respectively. These response contours can help in the prediction of the response for any zone of the experimental domain (Ref 20).

The apex of the response plot shows the maximum achievable shear strength and bonding strength. In Fig. 7 and 8, the shear strength and bonding strength increase with increasing bonding temperature, bonding pressure, and holding time and then decrease. But the shear strength and bonding strength increase with decreasing the surface roughness. A contour plot is produced to display the region of the optimal factor settings visually. For second-order responses, such a plot can be more complex compared to the simple series of parallel

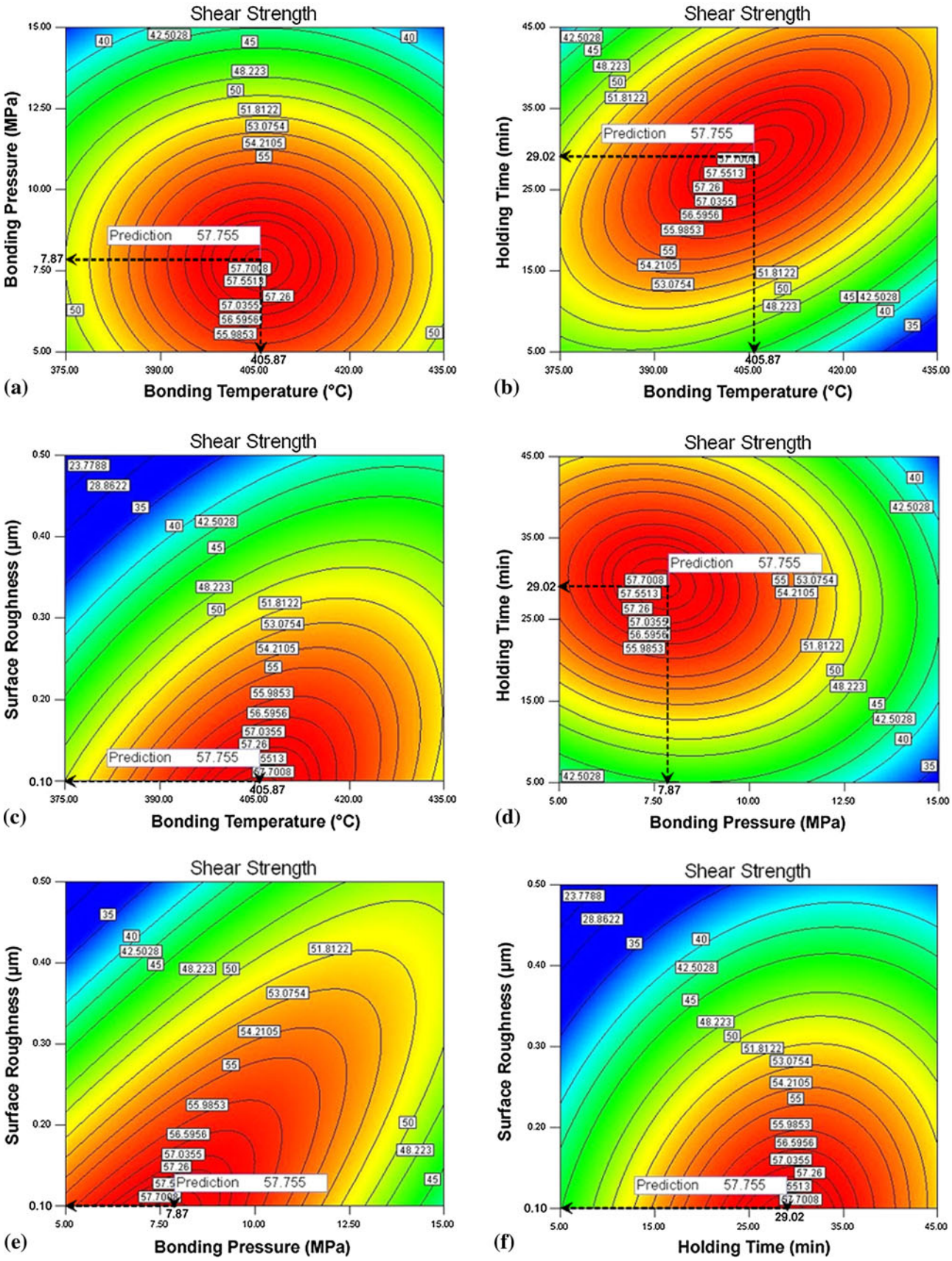

Fig. 9 Contour graphs for shear strength

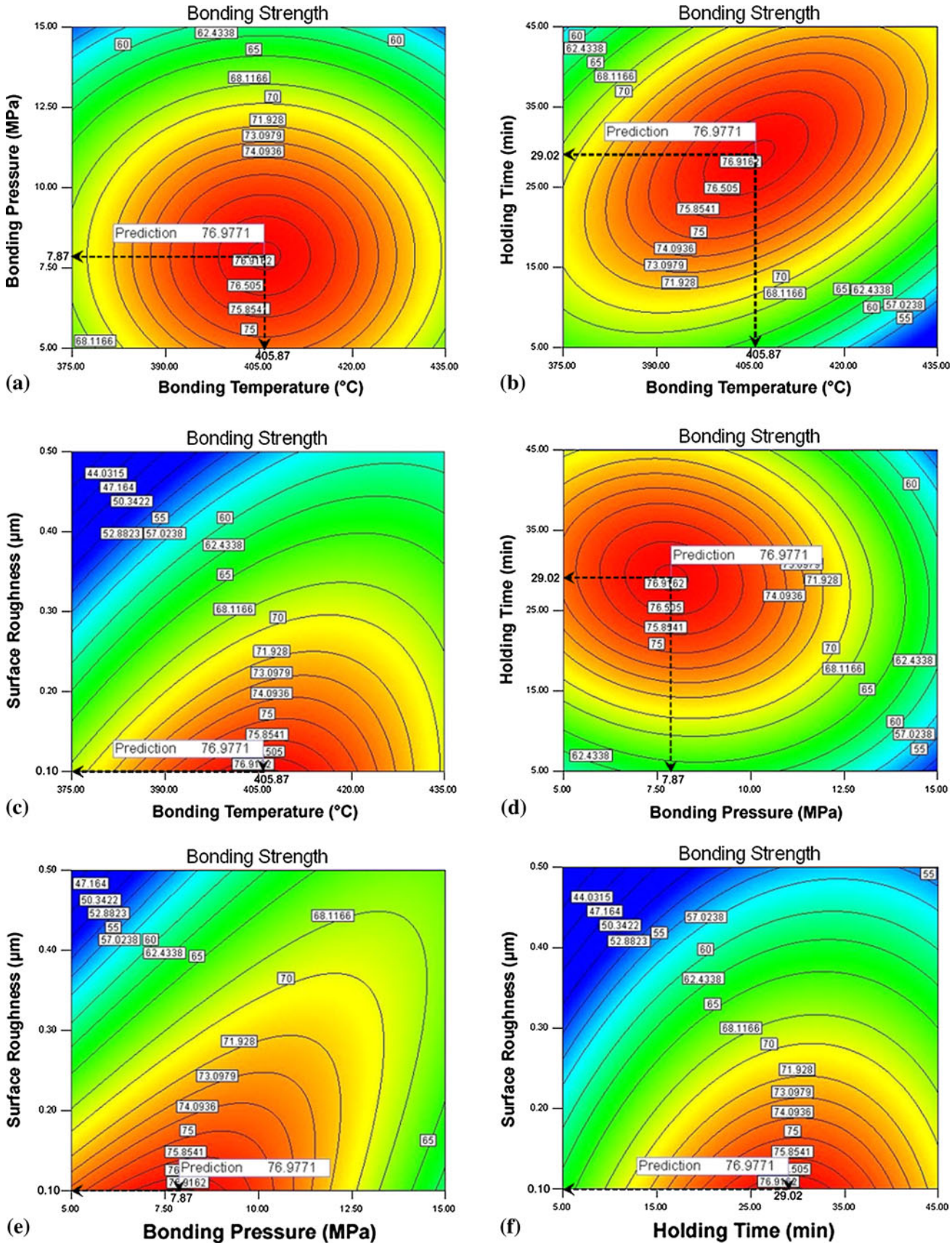

Fig. 10 Contour graphs for bonding strength

lines that can occur with first-order models. Once the stationary point is found, it is usually necessary to characterize the response surface in the immediate vicinity of the point. Characterization involves identifying whether the stationary point is a minimum response or maximum response or a saddle point. To classify this, it is most straightforward to examine it through a contour plot. Contour plots play a very important role in the study of a response surface. It is clear from Fig. 9 and 10 that the shear strength and bonding strength increase with the increase of bonding temperature, bonding pressure, holding time, and surface roughness to a certain value and then decrease.

Table 6 Estimated regression coefficients for shear strength and bonding strength

	Estimated regression coefficients	
Factor	**Shear strength**	**Bonding strength**
Intercept	53.5	70.66667
T	2.166667	2.166667
P	1.666667	1.666667
H	2.583333	2.583333
S	−3.41667	−3.75
T^2	−1.8125	−1.9375
P^2	−1.8125	−1.9375
H^2	−2.1875	−2.3125
S^2	−1.0625	−0.6875
TP	0	0
TH	2	2
TS	1.375	1.375
PH	−0.5	−0.5
PS	2.375	2.375
HS	0.625	0.625

RSM is used to find the optimal set of process parameters that produce a maximum or minimum value of the response (Ref 21). By analyzing the response surfaces and contour plots (Fig. 7 to 10), the maximum achievable shear strength and bonding strength values are found to be 57.70 and 76.90 MPa, respectively. The corresponding process parameters that yielded this maximum value are bonding temperature of 405.87 °C, bonding pressure of 7.87 MPa, holding time of 29.02 min, and surface roughness of 0.10 μm. Using these optimized diffusion bonding process parameters three more joints were fabricated. From these joints, lap shear and ram tensile specimens were fabricated and then tested. The average lap shear and bonding strength values are found to be 56 and 75 MPa. From these values, it is inferred that the predicted and experimental optimized strength values are in good agreement and the variations is found to be less than ±10%.

Contributions made by the process parameters on strength of the joint can be ranked (Ref 22) from their respective *F* ratio value which was presented in Table 6 provided the degrees of freedom are same for all the input parameters. The higher *F* ratio value implies that the respective term is more significant and vice versa. From the *F* ratio values, it can be concluded that bonding temperature is contributing more on shear strength and bonding strength, and it is followed by bonding pressure, holding time, and surface roughness for the range considered in this investigation.

5. Sensitivity Analysis

Sensitivity analysis, a method to identify critical parameters and rank them by their order of importance, is paramount in model validation where attempts are made to compare the

Table 7 Sensitivities of process parameters on shear strength (*S* = 0.1 μm)

Bonding pressure, P	Bonding temperature, *T*	Holding time, H	Shear strength, SS	∂SS/∂*T*	∂SS/∂*P*	∂SS/∂*H*	∂SS/∂*S*
5	375	5	23.42	−12.20	6.29	3.96	1.79
	390	15	11.82	−9.19	3.98	1.27	3.79
	405	25	26.21	−6.18	1.67	−1.42	5.79
	420	35	28.68	−3.17	−0.64	−4.11	7.79
	435	45	19.23	−0.16	−2.95	−6.80	9.79
7.5	375	5	11.51	−10.82	6.29	5.96	−0.02
	390	15	26.69	−7.81	3.98	3.27	1.98
	405	25	39.95	−4.80	1.67	0.58	3.98
	420	35	41.29	−1.79	−0.64	−2.11	5.98
	435	45	30.71	1.22	−2.95	−4.80	7.98
10	375	5	10.99	−9.44	6.29	7.96	−1.83
	390	15	35.04	−6.43	3.98	5.27	0.17
	405	25	47.17	−3.42	1.67	2.58	2.17
	420	35	47.38	−0.41	−0.64	−0.11	4.17
	435	45	35.67	2.60	−2.95	−2.80	6.17
12.5	375	5	13.95	−8.06	6.29	9.96	−3.64
	390	15	36.87	−5.05	3.98	7.27	−1.64
	405	25	47.87	−2.04	1.67	4.58	0.36
	420	35	46.95	0.97	−0.64	1.89	2.36
	435	45	34.11	3.98	−2.95	−0.80	4.36
15	375	5	10.39	−6.68	6.29	11.96	−5.45
	390	15	32.18	−3.67	3.98	9.27	−3.45
	405	25	42.05	−0.66	1.67	6.58	−1.45
	420	35	40.00	2.35	−0.64	3.89	0.55
	435	45	26.03	5.36	−2.95	1.20	2.55

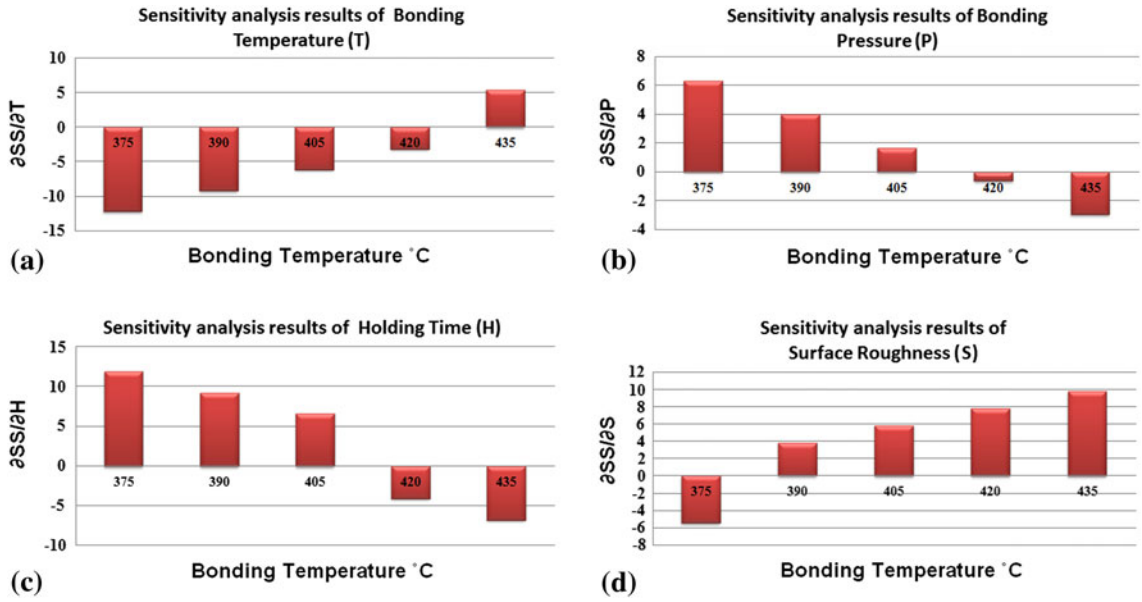

Fig. 11 Sensitivity analysis results. (a) Bonding temperature, (b) bonding pressure, (c) holding time, and (d) surface roughness

calculated output with the measured data. This type of analysis can be used to determine the parameters that must be accurately measured, thus knowing the input parameters exerting the most influence on the model response (Ref 23). Therefore, sensitivity analysis plays an important role in determining which parameter of the process should be modified to obtain the improved response characteristics. Mathematically, sensitivity of an objective function with respect to a design variable is the partial derivative of that function with respect to its variables (Ref 24).

In the present investigation, the aim is to predict the likely change in shear strength and bonding strength owing to a small change in process parameters for the diffusion bonding process. The sensitivity equations were obtained by differentiating the developed empirical relation with respect to the factors of interest such as bonding temperature, bonding pressure, holding time, and surface roughness, which were explored here. The sensitivity Eq 9, 10, 11, and 12 represent the sensitivity of shear strength for bonding temperature, bonding pressure, holding time, and surface roughness, respectively.

$$\partial \mathrm{SS}/\partial T = 2.17 + 0.00P + 2.00H + 1.38S - 3.62T \quad \text{(Eq 9)}$$

$$\partial \mathrm{SS}/\partial P = 1.67 + 0.00T - 0.50H + 2.38S - 3.62P \quad \text{(Eq 10)}$$

$$\partial \mathrm{SS}/\partial H = 2.58 + 2.00T - 0.50P + 0.63S - 4.38H \quad \text{(Eq 11)}$$

$$\partial \mathrm{SS}/\partial S = -3.42 + 1.38T + 2.38P + 0.63H - 2.12S \quad \text{(Eq 12)}$$

Sensitivity information should be interpreted using the mathematical definition of derivatives, namely positive sensitivity values imply an increment in the objective function by a small change in design parameter, whereas negative values state the opposite (Ref 22). Sensitivities of process parameters on shear strength are presented in Table 7. From Table 7, it is found that the maximum sensitivity values of bonding temperature, bonding pressure, holding time, and surface roughness are −12.20, 6.29, 11.96, and 9.79, respectively. Figure 11 shows the sensitivity of bonding temperature, bonding pressure, holding time, and surface roughness respectively on shear strength. The small variation of bonding temperature causes large changes in shear strength. The results reveal that the shear strength is more sensitive to bonding temperature than bonding pressure, holding time, and surface roughness. However, at 420 °C (Fig. 11a to c) and 390 °C (Fig. 11d) the sensitivity is found to be very small and this is mainly due to the change of magnitude of sensitivity (from positive to negative or vice versa). The sensitivity analysis for bonding strength will also show the same effect as it is directly proportional to the shear strength. Al/Al and Mg/Mg (similar) joints were fabricated using diffusion bonding method. The shear strength and bonding strength of Al/Al joints are found to be 155 and 185 MPa, respectively. Similarly, Mg/Mg joints yielded shear strength and bonding strength of 125 and 160 MPa, respectively.

6. Conclusions

The following important conclusions are obtained from this investigation

- Empirical relationships were developed to predict the shear strength and bonding strength of the diffusion bonded dissimilar joints of AZ80 magnesium and AA6061 aluminum alloys incorporating important parameters. The developed relationship can be effectively used to predict the shear strength and bonding strength of diffusion bonds at 95% confidence level.
- A maximum shear strength of 57.70 MPa and bonding strength of 76.90 MPa could be attained under the bonding conditions of 405.87 °C of bonding temperature, 7.87 MPa of bonding pressure, 29.02 min of holding time, and 0.10 μm of surface roughness. The experimentally determined shear strength and bonding strength at these

optimized parameters were found to be 56 and 75 MPa, respectively, which shows the consistency of the model.
- Bonding temperature was found to have greater influence on shear strength and bonding strength of the joints followed by bonding pressure, holding time, and surface roughness.
- Bonding temperature was more sensitive than the other parameters such as bonding pressure, holding time, and surface roughness. Therefore, a slight increase in bonding temperature induces a wide variation in the decrease in the strength of the dissimilar joints.

Acknowledgments

The authors are grateful to the Center for Materials Joining and Research (CEMAJOR), Department of Manufacturing Engineering, Annamalai University, Annamalai Nagar, India for extending the facilities of metal joining and Material Testing to carry out this investigation.

References

1. J. Wang, Y. Li, P. Liu, and H. Geng, Microstructure and XRD Analysis in the Interface Zone of Mg/Al Diffusion Bonding, *J. Mater. Process. Technol.*, 2008, **205**, p 146–150
2. P. Liu, Y. Li, H. Geng, and J. Wang, A Study of Phase Constitution Near the Interface of Mg/Al Vacuum Diffusion Bonding, *Mater. Lett.*, 2005, **59**, p 2001–2005
3. H. Somekawa, H. Watanabe, T. Mukai, and K. Higashi, Low Temperature Diffusion Bonding in a Super Plastic AZ31 Magnesium Alloy, *Scripta Mater.*, 2003, **48**, p 1249–1254
4. M.S. Yeh and T.S. Chuang, Low Pressure Diffusion Bonding of SAE 316 Stainless Steel by Inserting a Super Plastic Interlayer, *Scripta Metall. Mater.*, 1995, **33**(8), p 1277–1281
5. J.C. Feng, B.G. Zhang, Y.Y. Qian, and P. He, Microstructure and Strength of Diffusion Bonded Joints of Ti Al Base Alloy to Steel, *Mater. Charact.*, 2002, **48**, p 401–406
6. K.A. Peterson, I. Dutta, and M. Chenb, Processing and Characterization of Diffusion-Bonded Al-Si Interfaces, *J. Mater. Process. Technol.*, 2004, **145**, p 99–108
7. Y. Li, P. Liu, J. Wang, and H. Ma, XRD and SEM Analysis Near the Diffusion Bonding Interface of Mg/Al Dissimilar Materials, *Vacuum*, 2008, **82**, p 15–19
8. G. Mahendran, V. Balasubramanian, and T. Senthilvelan, Developing Diffusion Bonding Windows for Joining AZ31B Magnesium-AA2024 Aluminium Alloys, *Mater. Des.*, 2009, **30**, p 1240–1244
9. M. Joseph Fernandus, T. Senthilkumar, and V. Balasubramanian, Developing Temperature-Time and Pressure-Time Diagrams for Diffusion Bonding AZ80 Magnesium and AA6061 Aluminium Alloys, *Mater. Des.*, 2011, **32**, p 1651–1656
10. G. Mahendran, V. Balasubramanian, and T. Senthilvelan, Influences of Diffusion Bonding Process Parameters on Bond Characteristics of Mg-Cu Dissimilar Joints, *Trans. Non-Ferrous Met. Soc. China*, 2010, **20**, p 997–1005
11. G. Mahendran, V. Balasubramanian, and S. Babu, Optimising Diffusion Bonding Process Parameters to Attain Maximum Strength in Al-Cu Dissimilar Joints Using Response Surface Methodology, *Int. J. Manuf. Res.*, 2010, **5**, p 181–198
12. J. Grum and J.M. Slabe, The Use of Factorial Design and Response Surface Methodology for Fast Determination of Optimal Heat Treatment Conditions of Different Ni-Co-Mo Surfaced Layers, *J. Mater. Process. Technol.*, 2004, **155**, p 2026–2032
13. G. Mahendran, S. Babu, and V. Balasubramanian, Analyzing the Effect of Diffusion Bonding Process Parameters on Bond Characteristics of Mg-Al Dissimilar Joints, *J. Mater. Eng. Perform.*, 2010, **19**, p 657–665
14. S. Babu, K. Elangovan, V. Balasubramanian, and M. Balasubramanian, Optimizing Friction Stir Welding Parameters to Maximize Tensile Strength of AA2219 Aluminium Alloy Joints, *Met. Mater. Int.*, 2009, **15**(2), p 321–330
15. S. Rajakumar, C. Muralidharan, and V. Balasubramanian, Optimization of the Friction-Stir-Welding Process and Tool Parameters to Attain a Maximum Tensile Strength of AA7075-T_6 Aluminium Alloy, *J. Eng. Manuf.*, 2010, **224**, p 1175–1191
16. V. Gunaraj and N. Murugan, Application of Response Surface Methodology for Predicting Weld Bead Quality in Submerged Arc Welding of Pipes, *J. Mater. Process. Technol.*, 1999, **88**, p 266–275
17. M. Balasubramanian, V. Jayabalan, and V. Balasubramanian, Developing Mathematical Models to Predict Tensile Properties of Pulsed Current Gas Tungsten Arc Welded Ti-6Al-4V Alloy, *Meter. Des.*, 2008, **29**(1), p 92–97
18. P.K. Palani and N. Murugan, Optimization of Weld Bead Geometry for Stainless Steel Claddings Deposited by FCAW, *J. Mater. Process. Technol.*, 2007, **190**, p 291–299
19. L.M. Zhao and Z.D. Zhang, Effect of Zn Alloy Interlayer on Interface Microstructure and Strength of Diffusion-Bonded Mg-Al Joints, *Scripta Mater.*, 2008, **58**, p 283–286
20. C.L. Tien and S.W. Lin, Optimization of Process Parameters of Titanium Dioxide Films by Response Surface Methodology, *Opt. Commun.*, 2006, **266**, p 574–581
21. T.-H. Hou, C.-H. Su, and W.-L. Liu, Parameters Optimization of a Nano-Particle Wet Milling Process Using the Taguchi Method, Response Surface Method and Genetic Algorithm, *Powder Technol.*, 2007, **173**, p 153–162
22. A.K. Lakshminarayanan and V. Balasubramaian, Comparison of RSM with ANN in Predicting Tensile Strength of Friction Stir Welded AA7039 Aluminium Alloy Joints, *Trans. Non-Ferrous Met. Soc. China*, 2009, **19**, p 9–18
23. A.S. Sarigul and A. Secgin, Study on the Application of the Acoustic Design Sensitivity Analysis of Vibrating Bodies, *Appl. Acoust.*, 2004, **65**, p 1037–1056
24. M. Jayaraman, R. Sivasubramanian, V. Balasubramanian, and A.K. Lakshminarayanan, Prediction of Tensile Strength of Friction Stir Welded A356 Cast Aluminium Alloy Using Response Surface Methodology and Artificial Neural Network, *J. Manuf. Sci. Prod. Res.*, 2008, **9**, p 45–60